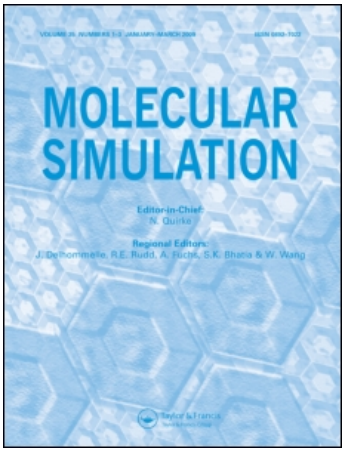

Molecular Simulation
Publication details, including instructions for authors and subscription information:
http://www.informaworld.com/smpp/title~content=t713644482

A Grand Canonical Monte-Carlo Study of Lennard-Jones Mixtures in Slit Pores; 2: Mixtures of Two Centre Ethane with Methane

Roger F. Cracknell[a]; David Nicholson[a]; Nicholas Quirke[b]
[a] Department of Chemistry, Imperial College of Science, Technology and Medicine, London, United Kingdom [b] European Centre for Computational Science and Technology, BIOSYM Technologies Sarl, Parc Club Orsay Université, Orsay, Cedex, France

To cite this Article Cracknell, Roger F. , Nicholson, David and Quirke, Nicholas(1994) 'A Grand Canonical Monte-Carlo Study of Lennard-Jones Mixtures in Slit Pores; 2: Mixtures of Two Centre Ethane with Methane', Molecular Simulation, 13: 3, 161 — 175
To link to this Article: DOI: 10.1080/08927029408021980
URL: http://dx.doi.org/10.1080/08927029408021980

Molecular Simulation, 1994, Vol. 13, pp. 161–175
Reprints available directly from the publisher
Photocopying permitted by license only

A GRAND CANONICAL MONTE-CARLO STUDY OF LENNARD-JONES MIXTURES IN SLIT PORES; 2: MIXTURES OF TWO CENTRE ETHANE WITH METHANE

ROGER F. CRACKNELL, DAVID NICHOLSON

Department of Chemistry, Imperial College of Science, Technology and Medicine, London SW72AY, United Kingdom

NICHOLAS QUIRKE

European Centre for Computational Science and Technology, BIOSYM Technologies Sarl, Parc Club Orsay Université, 20 rue Jean Rostand, 91893 Orsay Cedex, France

(Received October 1993, accepted March 1994)

Mixtures of ethane and methane in a slit micropore were simulated using the Grand Canonical Monte Carlo technique. Ethane was modelled as two Lennard-Jones sites while methane was modelled as a single Lennard-Jones site. The elongated shape of ethane was found to strongly influence the calculated adsorption selectivity, and important qualitative differences were noted relative to an earlier GCMC study (Cracknell *et al.*, *Molec Phys* Vol 80, pp 885–897, 1993) in which ethane was modelled as a spherical Lennard-Jones particle. The influence of ethane bond length on methane-ethane selectivity was studied further by conducting simulations with the ethane C–C distance 28% and then 70% longer than its actual length; the hindrance of rotation by confinement in the micropore was found to cause a significant decrease in selectivity. The Ideal Adsorbed Solution Theory was found to predict the selectivities with a reasonable degree of accuracy given simulated single component data as input.

KEY WORDS: Grand Canonical Monte-Carlo, ethane, methane, Ideal Adsorbed Solution Theory

1 INTRODUCTION

The viability of any process to separate gases by adsorption depends fundamentally on whether one gas is selectively adsorbed with respect to the other. It is obviously desirable to have a microporous material which possesses an optimum adsorption selectivity. The difficulties associated with obtaining clearly defined microporous systems suggest computer simulation as a useful approach in establishing the limitations and significant parameters in microporous adsorbents used for separations.

Both the molecular dynamics [1] and Monte-Carlo techniques of molecular simulation [2] [3] [4] [5] have been used to model physisorbed mixtures. Other workers have used Mean Field Density Functional Theory for the same purpose [1] [5] [6] [7] [8]. Density Functional Theories have the advantage of being computationally faster than full molecular simulations. In a previous paper [9], we have presented results for a Grand-Canonical Monte-Carlo study of Lennard-Jones

mixtures of methane and ethane in graphitic slit pores. Spherical Lennard-Jones models were used for both methane and ethane. In that paper we established a methodology for performing GCMC simulations of mixtures in an efficient manner by using particle interchange trials in addition to the familiar move, creation and deletion trials. The parameters used in the simulation were the same as in the density functional theory calculations of Tan and Gubbins [8]. In agreement with other comparisons of density functional theory and simulation, we found qualitative rather than quantitative agreement between the two methods, the discrepancy possibly being due to the mean field approximation used in the density functional theory. We also compared our simulation results with predictions made from the Ideal Adsorbed Solution Theory (IAST) [10] derived from single component isotherms of the model ethane and methane and found that the IAST worked well for the system under study.

Molecular simulations have proved of great value in elucidating the structure of the adsorbed monolayers of linear molecules such as nitrogen [11] [12], oxygen [13], carbon disulphide [14], carbon dioxide [15], chlorine [16], ethane [17], and ethylene [18] on graphite surfaces. However, there has been relatively little systematic study of non-spherical molecules in slit pores. Sokolowski studied a two centre Lennard-Jones model of oxygen in slit pores [19]; he demonstrated that molecules in the first adsorbed layer tend to lie either parallel or perpendicular to the wall, the relative distribution of orientations of molecules was found to depend strongly on pore size as well as on temperature and chemical potential.

In this work we extend of our previous study [9] to a more realistic model of ethane. We have used a two-centre Lennard-Jones model for ethane and a spherical Lennard-Jones model for methane. The principle object of this study is to examine the influence of ethane shape on selective adsorption in confined spaces. Calculations involving non-spherical particles are not amenable to density functional theory so that the present simulation study can not be compared with results from that approach. However, a further test of the IAS theory is possible: in simulations of mixtures in model zeolite cavities, Karavias and Myers [2] found that entropic effects arising from size differences of the adsorbate was the cause of deviations from ideality in the adsorbed phase, we have no *a priori* knowledge as to whether that result will apply to the system studied here.

2 METHOD

2.1 *Potentials*

Methane was modelled as a spherical Lennard-Jones site, ethane as two Lennard-Jones sites separated by a fixed bond length, l. The Lennard-Jones (12–6) potential is given by

$$u_{ij} = -4\,\varepsilon_{ij}\left[\left(\frac{\sigma_{ij}}{r_{ij}}\right)^6 - \left(\frac{\sigma_{ij}}{r_{ij}}\right)^{12}\right] \tag{1}$$

The interactions were cut (but not shifted) at 1.756 nm (5 times the ethane σ parameter) The parameters used in the simulation are given in table I. The model of ethane is due to Fischer [20] and has been shown to reproduce bulk thermodynamic properties reasonably accurately [21].

Table I Potential parameters used in the simulations.

Pair	*σ/nm*	*ε/k_B*	*l/nm*	*ref*
CH_4-CH_4	0.381	148.1 K	–	22
C_2H_6-C_2H_6(2CLJ)	0.3512	139.81 K	0.2353	20
C(graphite)-C(graphite)	0.340	28.0 K	–	22

The graphitic surface was treated as stacked planes of Lennard-Jones atoms. The interaction energy between a Lennard-Jones site on a fluid particle and a single graphite surface is given by the 10–4–3 potential of Steele [22]

$$u_{sf}(z) = 2\pi\rho_s\varepsilon_{sf}\sigma_{sf}^2\Delta\left\{\frac{2}{5}\left(\frac{\sigma_{sf}}{z}\right)^{10} - \left(\frac{\sigma_{sf}}{z}\right)^4 - \frac{\sigma_{sf}^4}{3\Delta(0.61\Delta + z)^3}\right\} \tag{2}$$

where Δ is the separation between graphite layers (=0.335 nm)and ρ_s is the number of carbon atoms per unit volume in graphite (114 nm^{-3}). σ_{sf} and ε_{sf} are the solid-fluid Lennard-Jones parameters which were calculated by combining the graphite parameters in table I with the appropriate fluid parameters using the Lorentz-Berthelot rules. The external field, $u^{(1)}$, in a slit pore of width H is the sum of the interaction with both graphitic surfaces and can be expressed mathematically as

$$u^{(1)} = u_{sf}(z) + u_{sf}(H - z) \tag{3}$$

(H is the C centre - C centre separation across the pore). Since our immediate interest here is in equilibrium adsorption at ambient temperatures, we have not accounted for the surface structure of the graphite planes on the pore walls. It should be stressed that a slit pore bounded by stacked parallel layers of graphite represents only a model of a porous carbon, and it is not clear that this is necessarily the best representation; for example some workers have considered a pore of triangular cross section to be a more appropriate representation of porous carbons [23].

2.2 *Comparison with experimental values of* q_{ST}^0

To test the potentials for the simulation, we calculated values for the isosteric heat of adsorption at zero coverage for both methane and ethane on a single graphitic surface using the relationship

$$q_{ST}^0 = RT - L\frac{\int_V u_S(\mathbf{r}, \boldsymbol{\omega})\exp(-\beta u_S(\mathbf{r}, \boldsymbol{\omega}))d\mathbf{r}d\boldsymbol{\omega}}{\int_V \exp(-\beta u_S(\mathbf{r}, \boldsymbol{\omega}))d\mathbf{r}d\boldsymbol{\omega}} \tag{4}$$

where L is Avogadro's constant and $u_S(\mathbf{r}, \boldsymbol{\omega})$ is the potential energy of interaction of a *molecule* in the pore, where $\mathbf{r}$ is the position of the centre of mass and $\boldsymbol{\omega}$ is the orientation. We used a Monte Carlo integration method with 1×10^7 trial insertions in order to evaluate (4), this number of trials was found to give isosteric heats with errors of less than 0.01%. In the limit of large H, there is no pore

Table II q^0_{ST} values; comparison of potentials used in this work versus experiment.

			$q^0_{ST}/kJ\ mol^{-1}$	
Ref for expt	*Adsorbate*	*T/K*	*Theoretical*	*Expt*
[24]	CH_4	300	10.2	12.7
[22]	CH_4	128	12.0	12.2
[24]	C_2H_6	300	18.6	16.0–19.7

enhancement effect and the potential represents two separate isolated graphitic surfaces; it was necessary to evaluate q^0_{ST} for single surfaces in order to facilitate unambiguous comparison with experimental data. Our results are summarised in table II

Lal and Spencer [24] have collected various literature values for isosteric heats, for ethane they give 4 values, our calculated value lies within the scatter of the experimental values. For methane on graphite, they give only one value which differs from our calculated value by 25%. The other literature value at 128 K agrees much better with our calculation at that temperature. Thus our potentials give calculated isosteric heats which are not inconsistent with literature values, we note that extant experimental data shows considerable scatter.

2.3 *GCMC Technique*

The GCMC method is ideally suited to adsorption problems because the chemical potential of each adsorbed species is specified in advance. The chemical potential can then be related to the external pressure by use of an equation of state or by running GCMC simulation of bulk homogeneous adsorbate. We note that the Isothermal-Isobaric (NPT) Monte-Carlo method has been successfully applied to the study of mixtures on a single surface [4], however extension to problems involving pores is problematic because the pressure tensor normal to the walls can not be equated to the bulk pressure.

As in our previous paper [9] we used four types of trial, specifically: attempts to move particles, attempts to delete particles, attempts to create particles and attempts to swap particle identities. A detailed discussion of the method is given in reference [9]. The simulations were run for 5×10^6 configurations on Intel i860 processors in a Transtech "parastation" with a PC front end acting as host. The simulations took between 2–4 hours for a single point depending on the number of particles in the system. The results reported in this paper were run using software developed at Imperial College, it was found to give identical results to software developed independently at ECCSAT.

3 RESULTS AND DISCUSSION

3.1 *Selectivity Isotherms*

We use the conventional definition of selectivity [25], as the ratio of the mole fractions in the pore to the ratio of the mole fractions in the bulk, thus the selectivity of ethane over methane is defined as

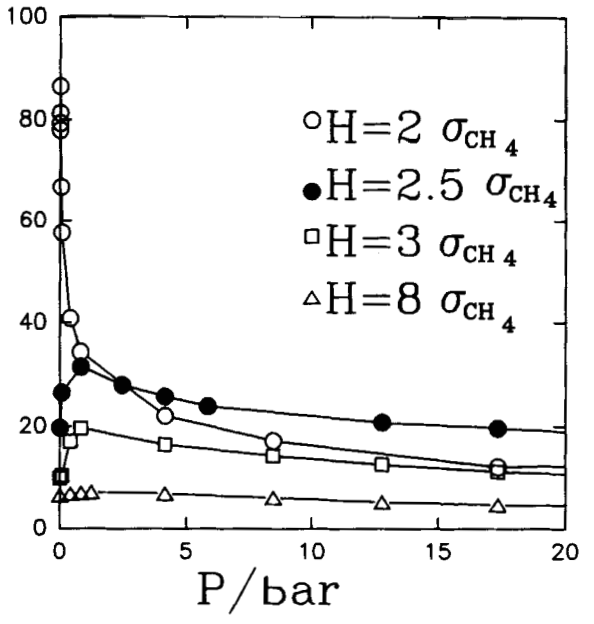

Figure 1 Ethane/methane selectivity for various pore widths. $y_e = 0.5$. $T = 296.2$ K.

$$S = \frac{x_e/x_m}{y_e/y_m} \tag{5}$$

where x_e and x_m are the pore mole fractions of ethane and methane respectively, and y_e and y_m, the respective bulk mole fractions of the gases.

Figure 1 shows the selectivity versus pressure for various pore sizes at 296.2 K with a bulk mole fraction of 0.5 [Strictly speaking the state points were generated with each component having the same absolute activity; at higher bulk pressure some densification of ethane relative to methane in the bulk occurs, thus for example at a pressure of 22 bar with equal bulk absolute activities, y_e is 0.535 rather than 0.5. Density functional calculations [8] show weak dependence on mole fraction over wide range]. The input chemical potentials were converted to bulk pressures, either using the ideal gas relationship:

$$P_i = \frac{\exp(\mu_i/kT)kT}{\Lambda_i^3} \tag{6}$$

(where P_i is the partial pressure corresponding to chemical potential μ_i and Λ_i is the thermal de Broglie wavelength of i.) or by running a grand canonical Monte Carlo simulation of bulk homogeneous adsorbate and calculating the pressure via the virial theorem.

All the selectivity isotherms in Figure 1, would be referred to as type I in the classification scheme of Tan and Gubbins [8], with the selectivity going through a

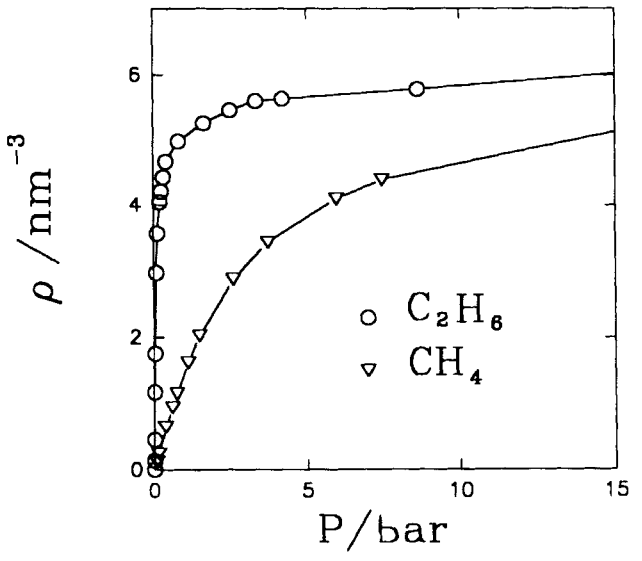

Figure 2 Single component isotherms for methane and ethane. Pore width $H = 2.5\,\sigma_{CH4}$, $T = 296.2$ K.

maximum before decaying with additional pressure. We note also a complicated dependence of selectivity on pore size, which will be discussed further in section 3.3

3.2 *Comparison with IAST*

The Ideal Adsorbed Solution Theory IAST [10] is essentially an application of Raoult's law to adsorbed phases. For a given component i, we can write

$$Py_i = P_i^0(\pi)x_i \tag{7}$$

where y_i and x_i are the bulk and pore mole fractions of i respectively, P is the total bulk pressure and $P_i^0(\pi)$ is the bulk pressure corresponding to spreading pressure π in the single component isotherm of component i. For a pore of width $H/\sigma_{CH4} = 2.5$ we used GCMC to generate single component isotherms for methane and ethane (Figure 2) for which P_i^0 and π are related according to

$$\pi(P_i^0) = \frac{RT}{A}\int_0^{P_i^0} n_i^0(p)d\ln p \tag{8}$$

It is possible for example to calculate x_i for a given P and y_i by first solving for $P_i^0(\pi)$ in the equation

$$\sum_i \frac{Py_i}{P_i^0(\pi)} - 1 = 0 \tag{9}$$

This equation follows from (7) since the sum of the mole fractions in the pore must equal unity.

We used two different types of fitting function for the single component data, firstly a Langmuir-Freundlich (LF) isotherm of the form,

$$n_i(P) = X\frac{(KP)^{\alpha}}{1 + (KP)^{\alpha}} \tag{10}$$

The advantage of using an LF fit is that integral in (8) can be carried out analytically to give

$$\pi(P) = \frac{RTX}{A\alpha}\ln(1 + (KP)^{\alpha}) \tag{11}$$

however, as Myers has noted [26], the LF equation has an incorrect low pressure (Henry's law) limit. This is an important deficiency because it is the loading *divided* by the pressure which is integrated with respect to pressure in (8) and the low pressure region makes a substantial contribution to the integral. As an alternative, we fitted the single component data to the Langmuir-Uniform-Distribution (LUD) equation which is the Langmuir isotherm modified for a patchwise heterogeneous surface,

$$n(P) = \frac{m}{2s}\ln\left[\frac{1 + CP\exp(s)}{1 + CP\exp(-s)}\right] \tag{12}$$

Like the Langmuir Freundlich equation, equation (12) has three adjustable parameters (C, s and m), however it does reduce to the correct Henry's law limit. Unfortunately the integral to determine the spreading pressure can not be done analytically. We adopted essentially the algorithm suggested by Myers in the appendix to reference 26 in order to use the LUD equation in the IAST: a subroutine employs a Newton-Raphson method to calculate P_i^0 corresponding to a particular π, while the main routine uses a Newton-Raphson method to solve (9).

It can be seen in Figure 3, that the both methods for implementing the IAS give results which are in reasonable agreement with the mixture simulations, the LUD method is superior to the Langmuir Freundlich method. We refitted the Langmuir Freundlich parameters giving additional weighting to the low pressure data points - the modified fit gave IAS predictions (not shown) that lay between the original LF and the LUD predictions for the range of pressures in Figure 3.

3.3 *The Effect of Pore Size on Selectivity*

Figure 4 shows selectivity versus pore size at 296.2 K for both the limit of zero pressure and a pressure of 12.8 bar. In the limit of zero pressure, the mole ratio in the pore (and hence the selectivity, since the bulk gases would be ideal in this limit) is given by the ratio of the 1 particle partition functions for each component, thus

$$S^0 = \frac{\frac{1}{4\pi}\int_V \exp(-\beta u_S^{ETHANE}(r,\omega))\,dr d\omega}{\int_V \exp(-\beta u_S^{METHANE}(r))\,dr} \tag{13}$$

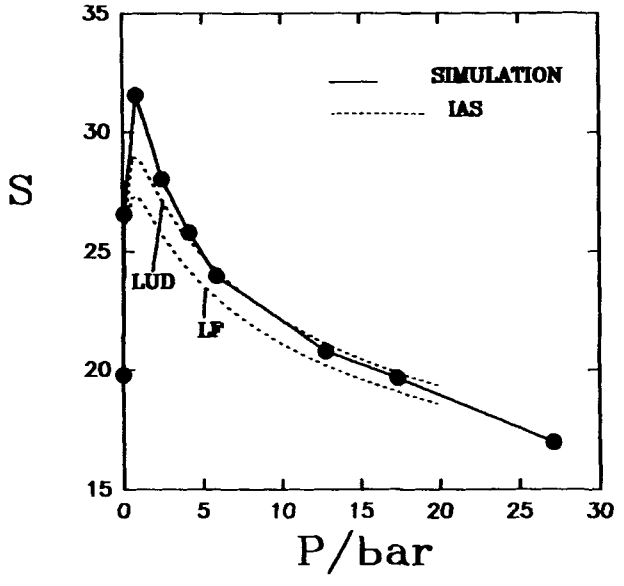

Figure 3 Comparison of simulation and Ideal Adsorbed Solution Theory predictions of selectivity derived from simulated single component isotherms (shown in Figure 2). The single component isotherms were fitted using the Langmuir-Freundlich equation (LF) and the Langmuir Uniform Distribution (LUD). Pore width $H = 2.5\,\sigma_{CH4}$, $y_e = 0.5$. $T = 296.2$ K.

This was evaluated conveniently using Monte-Carlo integration. At a pressure of 12.8 bar, slit pores of width in the range considered are always filled, the selectivities were calculated by the GCMC mixture method used in section 2.3.

The zero pressure plot shows a single maximum. The selectivity decreases to the right of the maximum because the depth of the potential wells become less. The selectivity decreases to the left of the maximum because of a molecular sieving effect. The calculations at 12.8 bar were considerably more computationally intensive than those necessary to evaluate (13). Consequently no simulations were run for very narrow pores, although it is to be presumed that there would be a molecular sieving effect. There are clearly discernible oscillations of selectivity with increasing pore size for the filled pore although the general trend is for selectivity to decrease. To gain an insight into the structural features of the adsorbed phase which give rise to these phenomena, we have plotted distribution functions (Figure 5) and snapshots (Figure 6) of pores of width $H/\sigma_{CH4} = 2.0$, 2.5, 3.0 and 3.6. The distribution functions are plotted for ethane only and refer to the position, r, of the centre of mass of the molecule from the centre of the pore. In the angular distribution function, θ is the angle between the bond in the ethane molecule and the normal to the pore wall, thus if $\langle\cos^2\theta\rangle$ is equal to 1, all molecules at a given r are perpendicular to the wall, conversely if $\langle\cos^2\theta\rangle = 0$, all molecules are parallel to the wall.

For the pore of width $H/\sigma_{CH4} = 2.0$, the molecules are confined to the centre of the pore and the ethanes are sterically constrained to lie flat. At $H/\sigma_{CH4} = 2.5$ there are two ways in which ethane molecules can have both methyl groups in the potential well at a pore wall; there is a central maximum in the density profile of

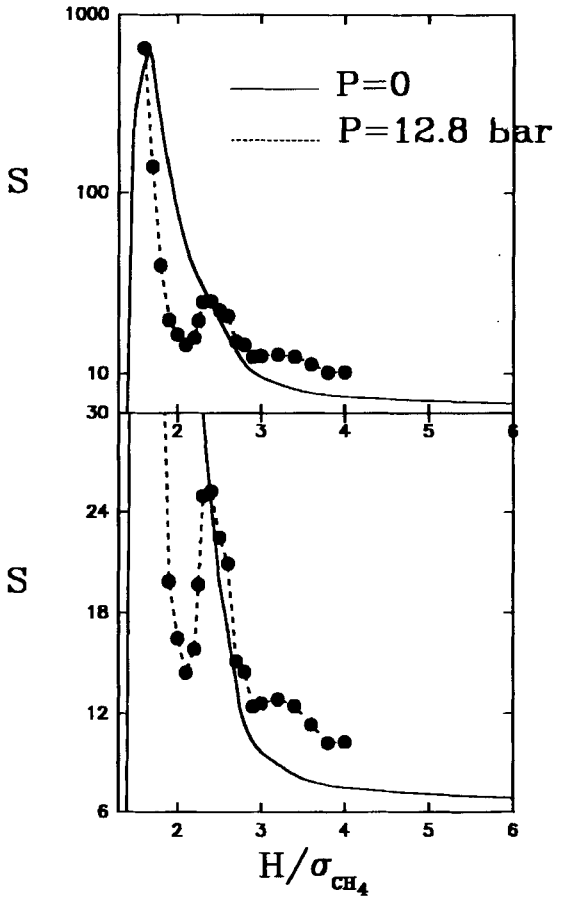

Figure 4 Ethane-methane selectivity versus pore width for zero pressure and $P = 12.8$ bar. $T = 296.2$ K. $y_e = 0.5$. Plotted on logarithmic (top) and linear (bottom) scales.

Figure 5(b) corresponding to ethanes spanning the pore and another maximum associated with those molecules which lie flat against the wall, this is also clearly illustrated in the snapshot, Figure 6(b). A similar mixture of "parallel" and "vertical" molecules has been noted by Sokolowski in his simulations of oxygen in slit pores [19]. For a pore of width $H/\sigma_{CH4} = 3.0$, the ethane molecules lie flat against the wall in two well defined layers. The reason why the pore of width $H/\sigma_{CH4} = 2.5$ corresponds to a maximum in selectivity is presumably because the interaction of the ethane with both walls is favoured by packing considerations. In our previous paper [9] we found for a spherical model of ethane and the same model of methane, that the pore of width $H/\sigma_{CH4} = 2.5$ actually corresponds to a *minimum* in selectivity, because the methane could pack neatly into two layers while the spherical ethane could not. Thus the elongated shape of this more realistic model for ethane is crucial in determining how selectivity varies with pore size. This issue is revisited in section 3.4. For a pore of width $H/\sigma_{CH4} = 3.6$ the adsorbate ordering is quite

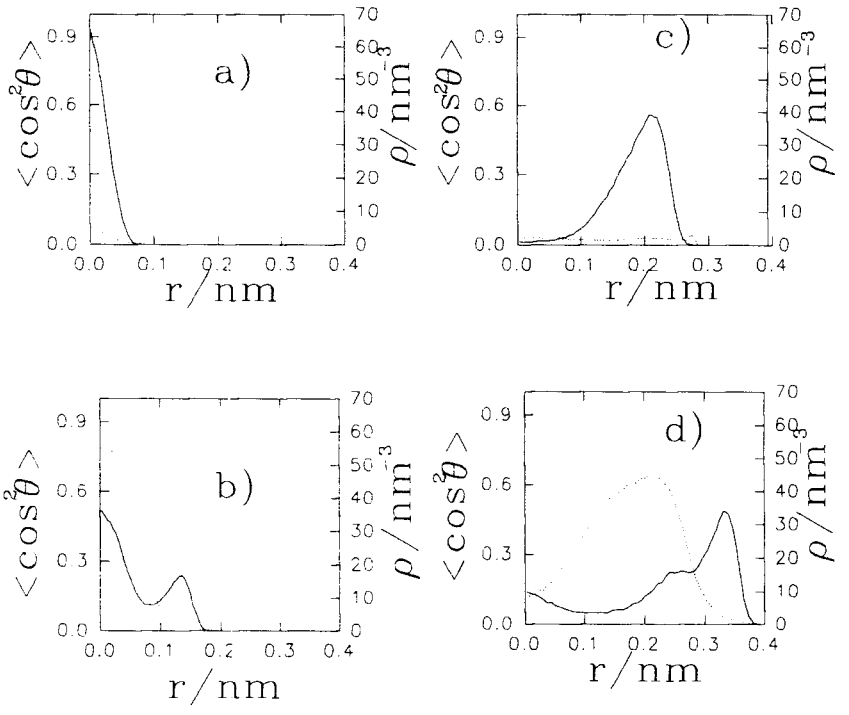

Figure 5 Density distribution (full line) and orientation distribution (dotted line) for the centre of mass of ethane molecules, plotted against the distance, r from the centre of the pore at 296.2 K and P = 12.8 bar for pores of width a) H/σ_{CH_4} = 2.0, b) H/σ_{CH_4} = 2.5, c) H/σ_{CH_4} = 3.0 d) H/σ_{CH_4} = 3.6. y_e = 0.5.

complex; there are layers of ethane lying flat against the wall and also in the centre of the pore but with some ethanes spanning the space between the layers against the wall and the central layer. This is the cause of the peak in the angle density profile.

3.4 *The Effect of Bond Length on Selectivity*

We investigated the influence of the ethane bond length on ethane-methane selectivity by elongating the molecule from the "normal" value of 0.235 nm to 0.3 nm and to 0.4 nm and calculating selectivity isotherms. We note that a bond length of 0.4 nm is unphysical and strictly speaking is not "ethane" at all. Figure 7 shows the pore mole fraction plotted against absolute activity ($z = \exp(\mu/kT)/\Lambda^3$) for various ethane lengths. Ignoring non-ideality (valid in the limit of low z_e), the sum of z_e and z_m can multiplied by 40.95 to give the pressure in bar and the selectivity can be equated with the pore mole fraction of ethane if the bulk mole fractions are both 0.5 in equation (6). For a given activity, the pore mole fraction of ethane decreases with elongation; if we focus on the low pressure (activity) limit, and consider the minimum energy configurations for each bond length, shown

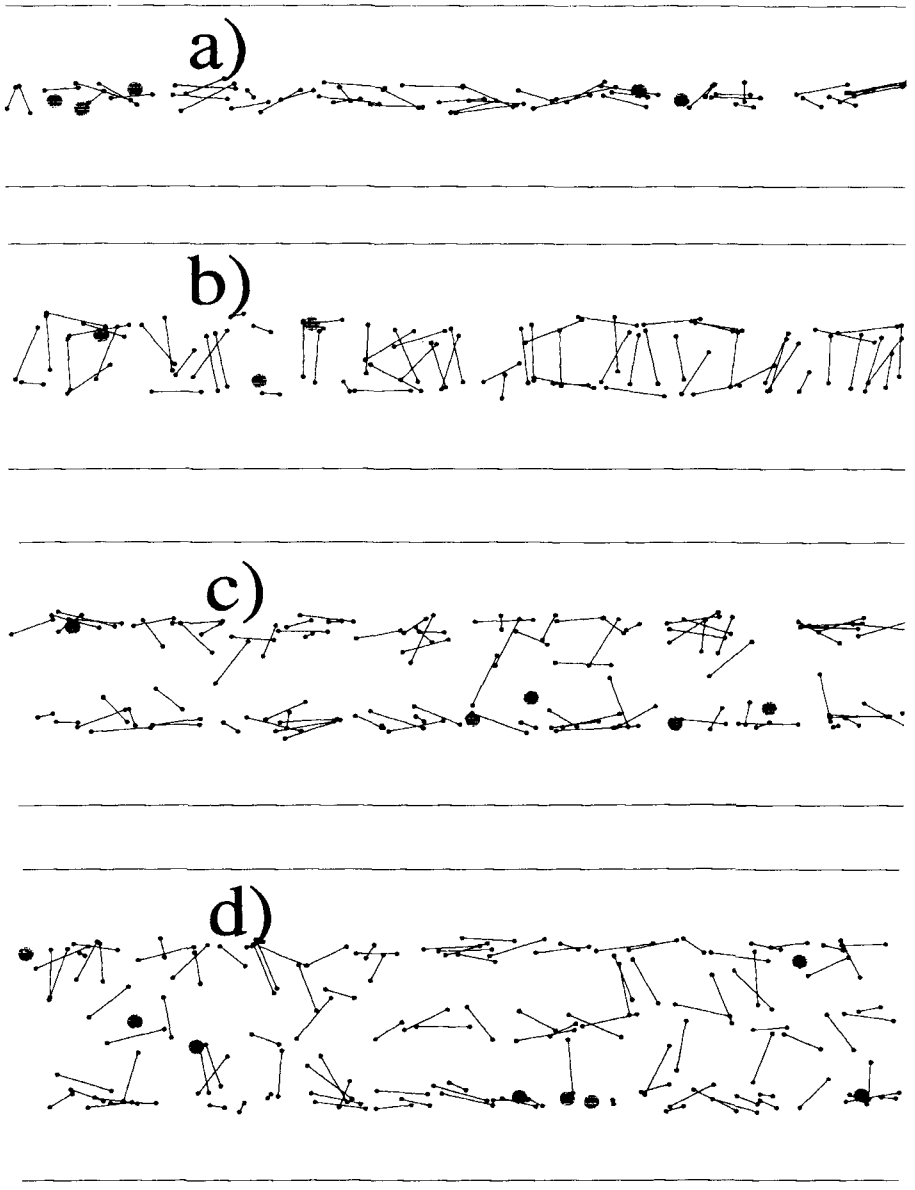

Figure 6 Snapshots at 296.2 K and P = 12.8 bar for pores of width a) H/σ_{CH4} = 2.0, b) H/σ_{CH4} = 2.5, c) H/σ_{CH4} = 3.0 d) H/σ_{CH4} = 3.6. The ethane molecules are shown as bonds, methane molecules as spheres (not drawn to scale).

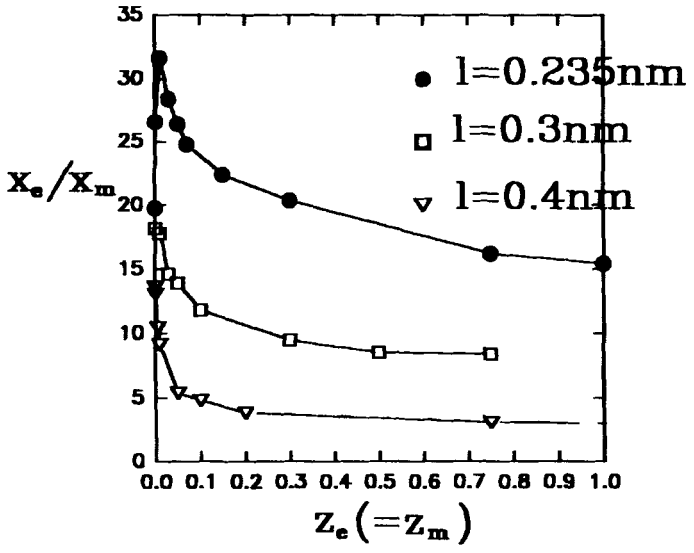

Figure 7 Effect of ethane elongation in a pore of width $H/\sigma_{CH4} = 2.5$. Pore mole fraction versus absolute activity of ethane. $z_e = z_m$, $T = 296.2$ K. The relationship between activity and pressure is discussed in the text.

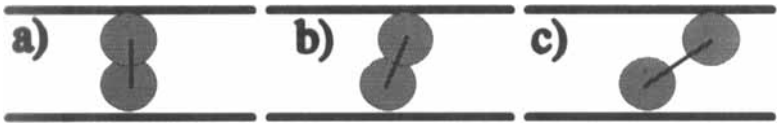

Figure 8 Minimum energy configurations (ie where a methyl group is in the potential minimum of each wall) for ethanes of bondlength a) 0.235 nm, b) 0.3 nm and c) 0.4 nm in a pore of width $H/\sigma_{CH4} = 2.5$ (0.9525 nm)

diagrammatically in Figure 8, it is clear that the minimum energy will be independent of bond length provided that both methyl groups are in the potential minimum of a pore wall. In the numerator of equation (13), with the centre of mass of the ethane in the middle of the pore, consider integration over the angular component. For case a) in Figure 8 all orientations will make a contribution to the integral, for case b), some configurations (ie those where the angle between bond and the normal to the pore wall is small) will make a zero contribution due to repulsive overlap with the walls - in case c) an even higher proportion of orientations will have a repulsive overlap and consequently make a zero contribution to the integral leading to a lower selectivity of ethane over methane.

It is also worth noting that the pressure (activity) dependence of selectivity varies with bond length, the 0.4 nm "ethane" molecule has a selectivity at $z_e = z_m = 1.0$ which is only a third of its value in the low pressure limit whereas, for a less elongated molecule, the selectivity does not decay as much (as a proportion) with

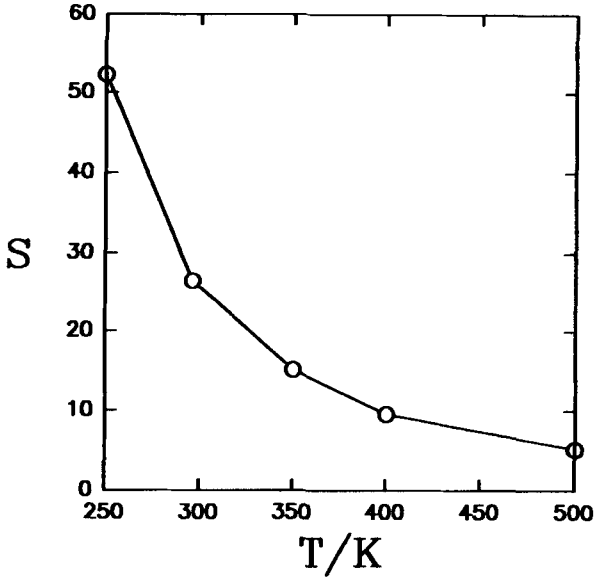

Figure 9 Ethane-Methane selectivity versus T. $H/\sigma_{CH4} = 2.5$, $y_e = 0.5$, $P = 4.1$ bar.

increased pressure(activity), indeed "real" ethane ($l = 0.235$ nm) shows a maximum in selectivity. These results are consistent with those depicted in Figure 1 where the effect of packing constraints on selectivity for pores of different width was demonstrated. We conclude that hindrance of rotation by confinement within a pore space can significantly reduce selectivity of the hindered species at zero coverage; this trend is augmented by steric effects associated with packing at higher concentrations.

3.5 *The Effect of Temperature on Selectivity*

We ran simulations at a pressure of 4.1 bar for a pore width $H/\sigma_{CH4} = 2.5$ with equal bulk mole fractions for temperatures in the range 200–500 K. Equation (13) suggests that selectivity would be expected to decay exponentially to zero with increasing temperature, and the results shown in Figure 9 do indeed confirm this expectation. While this temperature dependence is not too surprising, it is clear that heat management is likely to be of extreme importance for industrial adsorptive separation processes.

4.0 CONCLUSIONS

We have presented results for selective adsorption of a two centre Lennard-Jones model of ethane and a spherical Lennard-Jones model of methane. Comparison with our previous work [9] suggests that the elongated shape of ethane strongly influences the pore-size dependence of selectivity. The absolute values of selectivities

we calculate in this work are higher than in reference 9, it is not clear that a comparison of absolute values is meaningful since neither the spherical potential used in that paper nor the potential used here was parameterised by use of adsorption data (although we show in this work that the simulated isosteric heats of adsorption using the present model give results which are consistent with experiment).

Ethane has a significant quadrupole (about 3/4 that of N_2) which we have ignored in this study - it is possible that were it included, modified structures (eg "T" shaped configurations of pairs) would be favoured even at the fairly high temperatures used in this work. This is an interesting future area of study.

The Ideal Adsorbed Solution Theory (IAST) can provide a quite accurate description of methane-ethane mixture adsorption, although Langmuir Freundlich fits to the single component isotherms give rise to errors because the isotherm does not have the correct low pressure limit. Adsorption selectivity decreases exponentially with temperature. We are currently investigating propane-ethane, propane-methane selectivities as well as ternary C1/C2/C3 mixtures and the results will appear in a future publication.

Acknowledgements

This project was funded under BRITE EURAM CONTRACT BREU-CT92-0568. The authors wish to thank Mr S. Tennison of BP for his helpful comments and encouragement. We also acknowledge Dr S.J. Zara and the staff of Transtech limited for their assistance with computer hardware.

References

[1] S. Sokolowski and J. Fischer, "Lennard-Jones Mixtures in Slit-like Pores: a Comparison of Simulation and Density Functional Theory". *Mol. Phys.*, **71**, 393 (1990).

[2] F. Karavias and A.L. Myers, "Monte Carlo Simulation of Binary Gas Adsorption in Zeolite Cavities", *Mol. Sim.*, **8**, 51 (1991).

[3] D.M. Razmus and C.K. Hall, "Prediction of Gas Adsorption in 5A Zeolites using Monte Carlo Simulation" *A.I.Ch.E Journal* **37**, 5, (1991).

[4] J.E. Finn and P.A. Monson, "Monte Carlo Studies of Selective Adsorption on Solid Surfaces: Adsorption from Vapour Mixtures", *Mol. Phys.*, **72**, 661 (1992).

[5] E. Kierlik, M. Rosinberg, J.E. Finn, and P.A. Monson, "Binary Vapour Mixtures Adsorbed on a Graphite Surface: A Comparison of Mean Field Density Functional Theory with results from Monte Carlo Simulations", *Molec. Phys.*, **75**, 1435 (1992).

[6] E. Kierlik and M.L. Rosinberg, "Density Functional Theory for Inhomogeneous Fluids: II Adsorption of Binary Mixtures", *Phys. Rev. A*, **44**, 5025 (1991).

[7] Z. Tan, U.M.B. Marconi, F. van Swol, and K.E. Gubbins, "Hard Sphere Mixtures near a Hard Wall", *J. Chem. Phys.*, **90**, 3704 (1989).

[8] Z. Tan and K.E. Gubbins, "Selective Adsorption of Simple Mixtures in Slit Pores - A Model of Methane-Ethane Mixtures in Carbon. *J. Phys. Chem.*, **96**, 845 (1992).

[9] R.F. Cracknell, D. Nicholson, and N. Quirke, "A Grand Canonical Monte Carlo Study of Lennard-Jones Mixtures in Slit Shaped Pores", *Molec. Phys.*, **80**, 185 (1993).

[10] A.L. Myers and J.M. Prausnitz, "Thermodynamics of Mixed-Gas Adsorption", *A.I.Ch.E Journal*, **11**, 121 (1965).

[11] J. Talbot, D.J. Tildesley, and W.A. Steele, "A Molecular Dynamics Simulation of Nitrogen Adsorbed on Graphite) *Molec. Phys.*, **51**, 1331 (1984).

[12] B. Kuchta and R.D. Etters, "Calculated Properties of Monolayer and Multilayer N_2 on Graphite", *Phys. Rev. B*, **36**, 3400, (1987).

[13] Y.P. Joshi and D.J. Tildesley, "Molecular Dynamics Simulation and Energy Minimization of O_2 Adsorbed on a Graphite Surface", *Surf. Sci.*, **166**, 169 (1986).
[14] Y.P. Joshi, D.J. Tildesley, J.S. Ayres, and R.K. Thomas, "The Structure of CS_2 Adsorbed on Graphite", *Molec. Phys.*, **65**, 991 (1988).
[15] K.D. Hammonds, I.R. McDonald, and D.J. Tildesley, "Computational Studies of Carbon-Dioxide Monolayers Physisorbed on the Basal Plane of Graphice", *Molec. Phys.*, **70**, 175.
[16] K.D. Hammonds, I.R. McDonald, and D.J. Tildesley, 1993, "Computational studies of the Structure of Monolayers of Chlorine Physisorbed on the Basal Plane of Graphite", *Molec. Phys.*, **78**, 173 (1993).
[17] M.A. Moller and M.L. Klein "A Molecular Dynamics Study of the Low Temperature Structure and Dynamics of Ethane Monolayers Physisorbed on the Graphite Basal Plane". *J. Chem. Phys.*, **90**, 1960 (1989).
[18] M.A. Moller and M.L. Klein, "The Low Temperature Structure of Ethylene Monolayers Physisorbed on the Graphite Basal Plane", *Can. J. Chem.*, **66**, 2284 (1988).
[19] S. Sokolowski, "Adsorption of Oxygen in Slit-like pores: Grand Canonical Ensemble Monte Carlo studies" *Molec. Phys.*, **75**, 999 (1992).
[20] J. Fischer, R. Lustig, H. Breitenfelder-Manske, and W. Lemming "Influence of Intermolecular Potential Parameters on Orthobaric Properties of Fluids Consisting of Spherical and Linear Molecules". *Molec. Phys.*, **52**, 485 (1984).
[21] R. Lustig, A. Torro-Labbe, and W.A. Steele; "A Molecular Dynamics Study of the Thermodynamics of Liquid Ethane", *Fluid Phase Equilibria* **48**, 1 (1989).
[22] W.A. Steele, *The Interaction of Gases with Solid Surfaces* (Pergamon, Oxford) (1974).
[23] M. Bojan and W.A. Steele, "Molecular Motion in Krypton Films Physisorbed on a Grooved Graphite Surface - A Computer Simulation Study", *Ber. Buns. Ges. Phys. Chem.*, **94**, 300 (1990).
[24] M. Lal and D. Spencer, "Interactions of Alkanes with Graphite" *J. Chem. Soc. Faraday Trans. II*, **70**, 910 (1973).
[25] D.M. Ruthven, *Principles of Adsorption and Adsorption Processes*, (Wiley, New York, 1984).
[26] A.L. Myers, "Adsorption of Pure Gases and Their Mixtures on Heterogeneous Surfaces", in *Fundamentals of Adsorption*, A.L. Myers and G. Belfort, eds (Engineering Foundation, New York, 1984).

Note added in Proof:

The quantity, π, in equations 7 through 11, should not strictly speaking be termed the spreading pressure, since in equation (8), the quantity is calculated by integrating the total number of molecules in the pore, rather than the excess number with respect to d ln p. The IAS theory results shown in Figure 3 are nonetheless correct. The effect of using excess quantities in the IAS will be discussed in detail in a future publication.